

Photonic Crystal Fiber Based Refractive Index Sensors

K. Nazeri*, V. Ahsani*, F. Ahmed*, P.C. Lee**, and M.B.G. Jun***

*University of Victoria, Victoria, BC, Canada, fahmed@uvic.ca, ahsaniv@uvic.ca, nazerik@uvic.ca

**University of Vermont, Burlington, VT, USA, patrickc.lee@uvm.edu

***Purdue University, West Lafayette, IN, USA, mbgjun@purdue.edu

ABSTRACT

In this work two methods of making Mach-Zehnder Interferometer (MZI) for sensitive ambient refractive index (IR) measurement have been proposed by using photonic crystal fiber (PCF). PCF-MZI is fabricated by fusion splicing a short length of PCF between two single-mode fibers (SMF) with fully collapsed air holes in splicing region. Consequently, the fundamental core mode of PCF can be coupled to cladding modes at the first coupling region and then re-coupled to the core mode at the second coupling region. Miniaturized MZI is constructed using sharply tapered PCF and influence of sharp-tapering of PCF is then studied. Sharp-tapering of PCF over a short length of PCF is utilized by using tiny flame geometry. Experimental results verifies that sharp-tapering has a greater impact on refractive index sensitivity enhancement compare to decreasing taper waist diameter. MZI with length of 3.8 mm and taper waist diameter of 65 μm shows RI sensitivity of 677 to the miniaturized MZI, two types of polymer-deposited PCF-MZI is fabricated. Chitosan with RI~1.54 and Polycaprolactone (PCL) with RI~1.15 was filled into the cladding air-holes of PCF using capillary force. Chitosan-filled PCF with length of 10 mm shows RI sensitivity of 198.6 nm/RIU for RI range of 1.3327-1.3556, 474.5 nm/RIU for RI range of 1.3556 to 1.3917 and 677.8 nm/RIU for RI range of 1.3917-1.4204.

Keywords: Refractive index sensing, PCF, PCF-MZI, polymer-filled PCF, fiber tapering.

1 INTRODUCTION

Unique properties of fiber optic interferometric sensors such as light weight, ability of high resolution detection and immunity to electromagnetic wave have made them better choice over conventional sensors. Researchers have investigated different properties of photonic crystal fiber such as frequency-range of single-mode operation [1], high birefringence [2], and large mode area [3]. PCF owes its waveguide properties to an arrangement of tiny and closely-spaced air holes which goes through the length of fiber [4]. Knowing the fact that regions with missing holes have higher effective refractive index is essential in understanding the guiding properties of PCF [5]. Generally in PCF, index difference between core mode and cladding

mode is larger than 0.01 [6]. This property will cause a large delay within a short length of PCF, while keeping optical attenuation of the cladding mode at relatively low level [7]. Additionally, having the possibility to fill the holes with functional gases or liquids, the guiding properties can be strongly modified [5, 8]. Practical devices have been made based on solution-filled PCFs such as polarization filters [9] and fiber sensors [10].

In addition to rapid development of PCF, new types of MZI have been proposed using different methods such as core mismatch splicing [11], cladding collapse [12], fiber tapering [13], and hollow-core fiber splicing [14]. Using a beam splitter, an incident light will split into two arms and then recombined by a second splitter. This recombined light will produce an interference fringe according to the optical path difference (OPD) of the two arms. In the case of using MZI for ambient RI sensing, the sensing arm is exposed to solution while the reference arm is kept isolated. Ambient RI changes the OPD of MZI and variation in the interference pattern can be quantified.

The first PCF-MZI was proposed by MacPherson et al. [15]. Moreover, tapered PCF-MZI sensor was proposed by Lie et al. with sensing length of 2.4 cm and taper waist diameter of 30 μm in order to achieve RI sensitivity of 1600 nm/RIU [16]. Too much reduction in taper waist can cause reduction in rigidity of the sensor. Acid etching of PCF was also reported for sensing applications in which short length of sensor is required [17]. As mentioned above, it is possible to make interference between the core mode and cladding modes of PCF. By placing two coupling regions along the PCF and using collapse-method, MZI sensors in SMF-PCF-SMF configuration have been demonstrated, as schematically shown on figure 1-a. This type of MZI usually shows sinusoidal interference spectra over a wide range of wavelength.

In order to improve refractive index sensitivity, two different methods of making PCF-MZI are reported in this work. The sensors are fabricated by fusion splicing PCF between two SMF with fully collapsed air holes at splicing region. This happens as the holey structure of PCF has lower softening point in comparison to SMF.

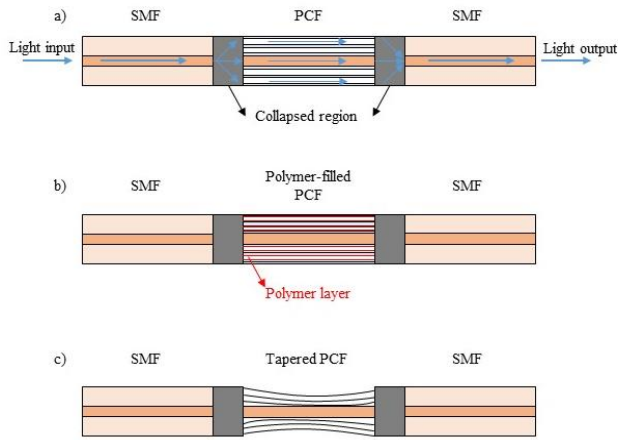


Figure 1. a) Schematic of a PCF-MZI; b) Polymer-filled PCF-MZI; c) Tapering of PCF.

In the first method by using a custom made tapering machine, miniaturized MZI is constructed by sharply tapering the PCF, while the SMFs on both sides remain unchanged. Figure 1-c shows a schematic view of the tapered PCF-MZI. Generally, a sensor with smaller PCF diameter shows higher sensitivity to ambient refractive index as it allows the cladding modes to extend much closer to the solution. All sensors were characterized with different concentration of glycerin solution and the influence of sharp-tapering on PCF-MZI is studied. Results shows that sharper tapering over a shorter length of PCF offer significantly higher RI sensitivity. The PCF-MZI with taper waist diameter of $65\ \mu\text{m}$ and length of 3.8 mm shows RI sensitivity of $334\ \text{nm}/\text{RIU}$ for RI range of 1.3327-1.3634, $673\ \text{nm}/\text{RIU}$ for RI range of 1.3634-1.3917 and $1426.7\ \text{nm}/\text{RIU}$ for RI range of 1.3917-1.4204. It is possible to tune the birefringence of PCF by changing refractive indices of solution in the air holes. In the second method, the cladding air holes of PCF were first filled with Chitosan (high refractive index solution) and PCL (low refractive index solution) using capillary force, as shown of figure 1-b. Later, by splicing a short length of polymer-filled PCF between two SMFs the new configuration can be fabricated. The spectral response of interferometer is investigated in terms of wavelength shift. PCL-filled PCF-MZI showed RI sensitivity of $173\ \text{nm}/\text{RIU}$ for the RI range of 1.3327 to 1.3917 and $325\ \text{nm}/\text{RIU}$ for RI ranges 1.3767 to 1.4204. But the Chitosan-filled PCF-MZI exhibited a sensitivity of $198.67\ \text{nm}/\text{RIU}$ for the RI range of 1.3327 to 1.3478, $474.5\ \text{nm}/\text{RIU}$ for RI ranges 1.3556 to 1.3917 and $677.84\ \text{nm}/\text{RIU}$ for RI ranges 1.3917 to 1.4204.

2 SENSOR FABRICATION

Fibers used in these experiments are SMF28 (core diameter: $8.2\ \mu\text{m}$) and PCF (Newport F-SM10; core diameter: $10\ \mu\text{m}$). This type of PCF has 6 layers of air-holes

surrounding the solid core. First step in filling air-holes of PCF is to prepare polymer solutions. By mixing 0.5 gr chitosan with 8 mL acetic acid and 80 mL deionized water, the first polymer solution was prepared. For PCL, 4 gr of PCL was mixed with 80 mL chloroform. Then, a short length of stripped and cleaved PCF was glued to the tip of a needle. The needle was attached to a syringe and tip of PCF was immersed in polymer solution. In order to enhance the capillary force, pressure difference was also applied through the syringe. The tip was kept in solution for a day to ensure that the air-holes are filled properly. Figure 2 shows a microscopic image of solution-filled PCF. Afterwards, PCF was heated up in an oven at 250°C for 3 hours, in order to evaporate the solution so that only a very thin layer of polymer remains inside the air-holes. PCF-MZI sensors with different lengths were fabricated and the results of 10mm PCF are reported and compared in this paper. Fujikura fusion splicer was used to splice fibers (FSM 40PM). The optimum splicing condition for polymer-filled PCF was found to be exposure of an arc power of 45 bit for 1200 milliseconds. The length of collapsing region is $\sim 150\ \mu\text{m}$ with splicing-loss of about 5 db.

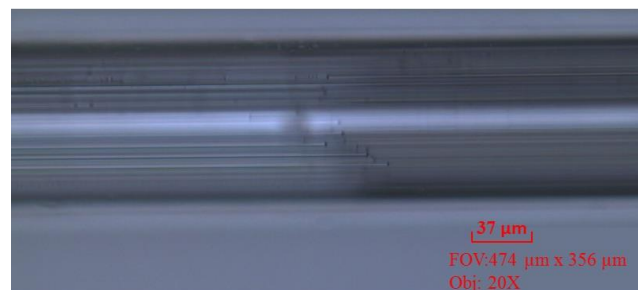


Figure 2. Microscope image of PCF filled with specified solution.

For the second experiment, custom made tapering machine was used to fabricate miniaturize MZI, as shown on fig 3.

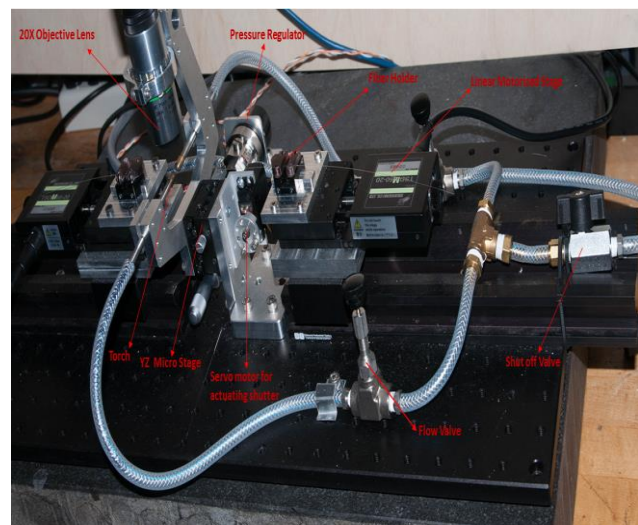


Figure 3. Details of the custom made tapering machine.

Fiber holders were mounted on linear stages driven by servomotor with resolution of $1\mu\text{m}/\text{pulse}$.

A converging-diverging nozzle with inner diameter of $50\mu\text{m}$ and outer diameter of $150\mu\text{m}$ was used. Hydrogen gas was fed into the nozzle at pressure of 20 PSI to produce a flame diameter of 1mm. The temperature of flame at the place that fiber passes was measured to be around $1100\text{ }^\circ\text{C}$. The splicing condition for SMF-PCF-SMF configuration was an arc power of 10 bit exposed for 1500 milliseconds. The first collapsed region splits the incoming core mode into core and cladding modes and then recombines them at the second collapsed region. Using this type of nuzzle and pulling the fiber at different speeds various sensors with different waist diameters and taper angles were fabricated. With the speed of $25\mu\text{m}/\text{s}$, MZI with taper waist diameter of $65\mu\text{m}$ and taper angle of 2.4° was fabricated, which is shown in figure 4. Sharp tapering and reduction in waist diameter enhances RI sensitivity of the sensor as it enables stronger mode interaction with ambient.

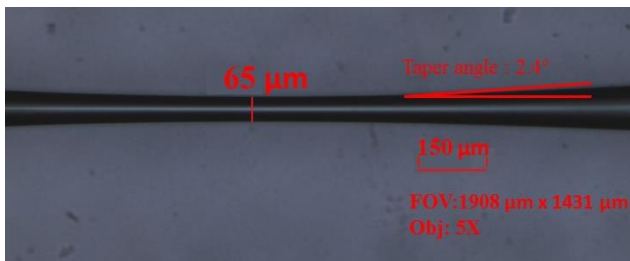


Figure 4. Microscope image of the taper morphology with taper diameter of $65\mu\text{m}$ and taper angle of 2.4° .

3 REFRACTIVE INDEX SENSING

Sensor performance is evaluated by its sensitivity, which is defined as wavelength shift divided by changes in ambient refractive index. For the case of tapered PCF, effective indices of core and cladding modes depend on waist diameter of tapered PCF. Additionally, interaction between evanescent field of the cladding mode and ambient solution varies the index of cladding mode. Sensors were characterized with different glycerin-solution concentrations at room temperature and after each step cleaned with deionized water. Figure 5 illustrates the wavelength shifts due to changes in surrounding refractive index between 1.3327 and 1.4204 for the normal PCF-MZI, polymer-filled and tapered sensors. Tapered sensors with different waist diameters were fabricated and the results were compared, but the results of tapered PCF-MZI with waist diameter of $65\mu\text{m}$ and tapering angle of 2.4° is reported in this article. It was concluded that sharp-tapering has a greater impact on refractive index sensitivity enhancement compare to decreasing taper waist diameter. As it is shown, tapered PCF-MZI shows much higher sensitivity compared to the other interferometers.

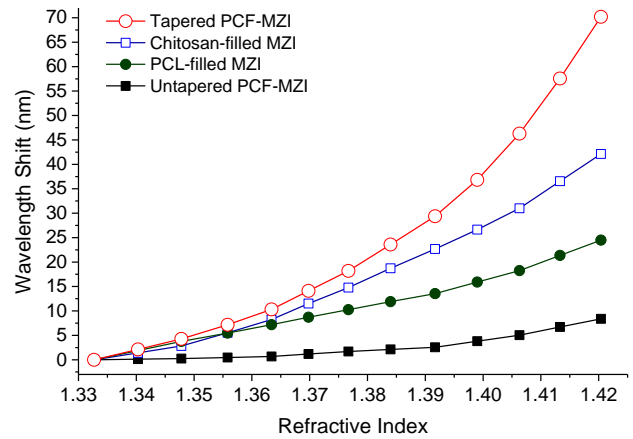


Figure 5. Refractive index sensitivity plots for a normal PCF-MZI, PCL-filled, chitosan-filled and tapered PCF based MZI sensors.

In order to compare the RI sensitivity of tapered and chitosan-filled PCF-MZI, their responses are divided into subplots shown in Figures 6. RI sensitivity of $90\text{ nm}/\text{RIU}$ for the IR range of 1.332 to 1.3634, $128\text{ nm}/\text{RIU}$ for RI range of 1.3634 to 1.3917 and $378\text{ nm}/\text{RIU}$ for range of 1.3917 to 1.4204 was obtained for normal PCF-MZI with PCF length of 10 mm. The PCL-filled with the same length of PCF showed RI sensitivity of $173\text{ nm}/\text{RIU}$ for RI range of 1.3327 to 1.3917 and $325\text{ nm}/\text{RIU}$ for the range of 1.3917 to 1.4204. As demonstrated in figure 6, chitosan-filled sensor with the same length showed RI sensitivity of $198.67\text{ nm}/\text{RIU}$ for the range of 1.3327 to 1.3478, $474.5\text{ nm}/\text{RIU}$ for RI range of 1.3478 to 1.3917 and $677.84\text{ nm}/\text{RIU}$ for RI range of 1.3917 to 1.4204. The tapered PCF-MZI with waist diameter of $65\mu\text{m}$ showed RI sensitivity of $334\text{ nm}/\text{RIU}$ for RI range of 1.3327 to 1.3634, $673\text{ nm}/\text{RIU}$ for range of 1.3634 to 1.3917 and $1426.7\text{ nm}/\text{RIU}$ for range of 1.3917 to 1.4204.

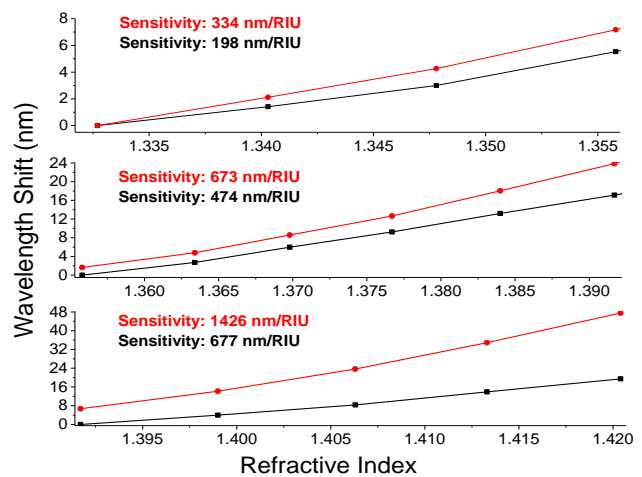


Figure 6. RI sensitivity analysis of tapered PCF-MZI and chitosan-filled MZI sensor.

4 CONCLUSION

Two sensitive RI sensor were proposed based on PCF using collapsing method. In addition to normal PCF-MZI, two types of polymer-filled sensors and tapered PCF-MZI were fabricated and their spectral responses were investigated. Sensors were characterized with different concentrations of glycerin. Results prove that by depositing thin layer of appropriate polymer inside the air holes, one could enhance the sensitivity of PCF-MZI. Chitosan-filled PCF shows the total wavelength shift of 42 nm due to changes in surrounding RI from 1.3327 to 1.4204. This sensor has RI sensitivity of 198.67 nm/RIU for the range of 1.3327 to 1.3478, 474.5 nm/RIU for RI range of 1.3478 to 1.3917 and 677.84 nm/RIU for RI range of 1.3917 to 1.4204.

Sharp-tapering over a short length of PCF was utilized by using a converging-diverging nozzle and a custom made tapering machine. Tapered sensor with waist diameter of 65 μm shows total wavelength shift of 70 nm. Additionally, it has the highest sensitivity with amount of 334 nm/RIU for RI range of 1.3327 to 1.3634, 673 nm/RIU for range of 1.3634 to 1.3917 and 1426.7 nm/RIU for range of 1.3917 to 1.4204. Based on the experiments it was concluded that sharp-tapering has a greater impact on refractive index sensitivity enhancement compare to decreasing taper waist diameter.

Acknowledgment

The authors acknowledge the support of Korea Carbon Capture and Sequestration Research and Development Center for this work.

REFERENCES

1. Knight, J.C., et al., *All-silica single-mode optical fiber with photonic crystal cladding*. Optics Letters, 1996. **21**(19): p. 1547-1549.
2. Chen, D. and L. Shen, *Highly Birefringent Elliptical-Hole Photonic Crystal Fibers With Double Defect*. Journal of Lightwave Technology, 2007. **25**(9): p. 2700-2705.
3. Ademgil, H. and S. Haxha, *Endlessly single mode photonic crystal fiber with improved effective mode area*. Optics Communications, 2012. **285**(6): p. 1514-1518.
4. Hao, R., et al., *Photonic crystal fiber with high birefringence and low confinement loss*. Optik - International Journal for Light and Electron Optics, 2013. **124**(21): p. 4880-4883.
5. Birks, T.A., J.C. Knight, and P.S.J. Russell, *Endlessly single-mode photonic crystal fiber*. Optics Letters, 1997. **22**(13): p. 961-963.
6. Jiangbing Du, Y.D., Gordon K. P. Lei, Weijun Tong, Chester Shu., *Photonic crystal fiber based MZI for DPSK signal demodulation*. Optical Society of America, 2010. **18**: p. 7917-7922.
7. Hu, L.M., et al., *Photonic Crystal Fiber Strain Sensor Based on Modified Mach-Zehnder Interferometer*. IEEE Photonics Journal, 2012. **4**(1): p. 114-118.
8. https://www.rp-photonics.com/photonic_crystal_fibers.html.
9. Xue, J., et al., *Polarization filter characters of the gold-coated and the liquid filled photonic crystal fiber based on surface plasmon resonance*. Optics Express, 2013. **21**(11): p. 13733-13740.
10. Wang, Y., et al., *Selectively Infiltrated Photonic Crystal Fiber With Ultrahigh Temperature Sensitivity*. IEEE Photonics Technology Letters, 2011. **23**(20): p. 1520-1522.
11. Chen, X., et al., *Temperature insensitive bending sensor based on in-line Mach-Zehnder interferometer*. Photonic Sensors, 2013. **4**(3): p. 193-197.
12. Choi, H.Y., M.J. Kim, and B.H. Lee, *All-fiber Mach-Zehnder type interferometers formed in photonic crystal fiber*. Optics Express, 2007. **15**(9): p. 5711-5720.
13. Lee, B.H., et al., *Interferometric fiber optic sensors*. Sensors (Basel), 2012. **12**(3): p. 2467-86.
14. Ming Deng, C.-P.T., Tao Zhu, Yun-Jiang Rao., *PCF-based Fabry-Pérot interferometric sensor for strain measurement at high temperatures*. IEEE PHOTONICS TECHNOLOGY LETTERS, 2011. **23**: p. 700-703.
15. MacPherson, W.N., et al., *Remotely addressed optical fibre curvature sensor using multicore photonic crystal fibre*. Optics Communications, 2001. **193**(1-6): p. 97-104.
16. Li, C., et al., *Ultra-Sensitive Refractive Index Sensor With Slightly Tapered Photonic Crystal Fiber*. IEEE Photonics Technology Letters, 2012. **24**(19): p. 1771-1774.
17. Qiu, S.-j., et al., *Miniature tapered photonic crystal fiber interferometer with enhanced sensitivity by acid microdroplets etching*. Applied Optics, 2011. **50**(22): p. 4328-4332.